Journal of Membrane Science 700 (2024) 122690

Contents lists available at ScienceDirect

Journal of Membrane Science

journal homepage: www.elsevier.com/locate/memsci

Unravelling the effects of surface modification pre-treatments on porous hastelloy X supports for H_2 selective Pd-based membranes preparation with a statistical approach

S. Agnolin [a], F. Gallucci [a,b,*]

[a] Inorganic Membranes and Membrane Reactors, Sustainable Process Engineering, Department of Chemical Engineering and Chemistry, Eindhoven University of Technology, De Rondom 70, Eindhoven, 5612 AP, the Netherlands
[b] Eindhoven Institute for Renewable Energy Systems (EIRES), Eindhoven University of Technology, PO Box 513, Eindhoven 5600, MB, the Netherlands

ARTICLE INFO

Keywords:
Support surface quality
Pd-based membranes
Metal supports
ANOVA

ABSTRACT

Metal-based supports require specific pre-treatments to reach the surface quality needed for achieving thin Pd layers deposition without defects. Hastelloy X supports with high surface roughness and large pore diameter are acquired and pre-treated via polishing and chemical etching. They are then asymmetrically filled with α-Al_2O_3 of decreasing particle size (18 μm, 5 μm and 1.5 μm) and equipped with a γ-Al_2O_3 interdiffusion barrier. Each pre-treatment step is thoroughly characterized and elucidated with ANalysis Of VAriance (ANOVA) as statistical tool, introducing a hybrid observational-statistical approach to infer on a population of membrane supports.

The analysis allowed to set average surface roughness (Ra) < 0.8 μm, average profile height (Rz) < 7 μm, in-pore leveling (Δ) < 6 μm, as targets for support pre-treatments reproducibility. The target average pore diameter after asymmetric filling was identified as 100–500 nm, while the target average pore diameter after interdiffusion barrier deposition was below 100 nm. The most effective particle size for in-pore leveling was identified as ≤ 5 μm, and the most effective particle size for average pore diameter reduction as 18 μm.

1. Introduction

Membrane reactors have emerged as promising alternative to conventional processes due to their ability to integrate reaction and separation in one single unit [1–3] This process intensification technique increases energy efficiency and promotes compactness of the equipment, reducing emissions and operational costs [4–6]. The insertion of membranes in the reaction environment promotes the continuous removal of the reaction product, shifting the equilibrium owing to Le Chatelier's principle. Specifically, for reactions in which H_2 is the desired product, Pd-based membranes have been widely investigated due to their unique solution diffusion H_2 transport mechanism [3,7,8]. This peculiar characteristic makes these membranes particularly suitable for membrane-assisted steam methane reforming [4,9,10], membrane-assisted ammonia decomposition [11–13] and membrane-assisted dehydrogenation applications [14,15].

To favor the membranes integration in the reactor, thin Pd films are deposited onto a suitable support. Most applications have been investigated by using ceramic supported Pd films, due to the ease of deposition given by the support's easily tailorable superficial characteristics (i.e., low surface roughness, average pore size ~100 nm) [16–18]. However, their sealing, integration when coupled to steel reactor structures, and resistance to solicitations remain challenging for scale up at high Technology Readiness Level (TRL) [19].

To overcome these challenges, metallic supported Pd membranes are investigated as an alternative [20–22]. However, the deposition of Pd films on metallic supports requires additional steps due to: 1) strong support-Pd interaction (known as metallic interdiffusion) [23–25], and 2) insufficient support's surface quality (i.e., high surface roughness, large superficial pore size ≥ 20 μm) [26,27]. It is therefore necessary to investigate suitable support pre-treatments to ease the deposition of Pd-based film [28,29].

In our previous work, a preparation procedure yielding to highly selective (H_2/N_2 ideal selectivity ~43200 at 400 °C, 1 bar) Pd–Ag membranes supported onto large media grade (0.5 μm) Hastelloy X porous tubes was developed. The development was carried out by

* Corresponding author.Inorganic Membranes and Membrane Reactors, Sustainable Process Engineering, Department of Chemical Engineering and Chemistry, Eindhoven University of Technology, De Rondom 70, Eindhoven, 5612 AP, the Netherlands.
E-mail address: f.gallucci@tue.nl (F. Gallucci).

https://doi.org/10.1016/j.memsci.2024.122690
Received 2 January 2024; Received in revised form 27 February 2024; Accepted 20 March 2024
Available online 22 March 2024

studying the support's surface morphology with a statistical method [30].

Statistical methods are often employed in membrane's performance assessment, where varying membrane reactor operating conditions such as temperature, pressure, feed flow, etc. results in an outcome on membrane separation performance [31–33]. Moreover, they are often applied whenever the selected type of membrane allows for a non-time-consuming preparation, when keeping all non-analyzed preparation parameters constant, or when solely a few parameters are expected to influence membrane performance (i.e. with polymer casting) [34–36]. However, when observing experimental sections in the literature of Pd-based/composite membranes preparation, trial-and-error or one factor at a time (OFAT) design of experiment methods are the most implemented [18,37–39]. These methods offer a rapid insight on which of the multitude of parameters in membrane preparation can be influential in final performance, with a non-time-consuming design. This approach implies that oftentimes solely the best performing membranes (resulting from the best combination of investigated factors) are presented [20–22,25,40–43]. However, a multitude of parameters can hinder the reproducibility of best results, especially if the applied preparation procedure includes intrinsically random steps (i.e. large differences between supports surface characteristics, wide support pore size distributions, variable surface roughness profile, etc.). Moreover, detection of differences in average values and characterization techniques of various preparation steps still require a certain degree of interpretation which is left to the experience of the experimenter. To fully analyze membrane preparation steps without observational bias, backing up observation with mathematical considerations, Design of Experiment (DoE) and statistical analysis techniques can be employed. One of the main objectives of DoE is to verify a hypothesis efficiently and cohesively, allowing the utilization of a suitable statistical technique for the data analysis to follow [44].

The ANalysis Of VAriance (ANOVA) technique, provided the data fulfills the necessary assumptions, can be used to test null hypothesis of equality of several means (testing the significance of means) of several independent groups of observations having the same variance [45]. It assesses potential differences in a continuous dependent variable given by one or more independent variables (factors) having two or more levels.

In this work, the characterization of surface modification techniques aimed at rendering highly rough Hastelloy X supports with large pore diameter suitable for Pd deposition via electroless plating is carried out for the first time with a hybrid observational-statistical approach. The supports are modified by polishing, etching, filling with α-Al_2O_3 particles of decreasing size and deposition of a γ-Al_2O_3 interdiffusion barrier. Subsequently, an elucidatory study of the main variables involved in surface modification of metallic supports for Pd-based membranes is carried out. Such variables and their evolution are investigated for each of the chosen support pre-treatments via suitable DoE, coupled with ANOVA as analysis tool. The pre-treatments are operated on a suitable sample of 20 supports, drawn from a population of supplied supports. Onto each support, a sample representative of a population of pores is drawn. The measurement and repetition of the same for morphological variables involved in each pre-treatment guarantees for the first time to study the effect of support pre-treatment steps on several equal samples, allowing for the correlation between the studied outcome variables and support reproducibility considerations, completed by setting suitable targets to ensure final supports with similar surface characteristics.

2. Experimental methods

2.1. Samples preparation

Four 50 cm long porous sintered Hastelloy X supports were acquired from Hebei Golden Flame Wire Mesh Co, China. The supports were cut in samples of 10 cm and welded to dense stainless-steel caps to achieve a one close end configuration, while the other side was welded to a dense stainless-steel tube, as per previous procedures [13,26,30]. The samples were then introduced in a vibratory polishing machine for a total amount of 6 h. They were then rinsed with deionized water and dried in a tubular furnace at 120 °C for 2 h. The dry samples were then submerged in fresh Aqua Regia for 30 s each. They were once again thoroughly rinsed inside and out with deionized water immediately after submersion to prevent the etching process from continuing. Finally, the supports were oxidized in a static air furnace at 750 °C for 1 h, with a heating ramp rate of 3 °C/min.

The supports were filled via dip-coating with a 10 wt% dispersion of α-Al_2O_3 of different particle sizes (18 μm, 5 μm) and for a different number of cycles (20, 30), according to the DoE described in the following sections. Finally, 5 selected supports were asymmetrically filled with spherical α-Al_2O_3 of decreasing size (18 μm, 5 μm, 1.5 μm). Onto these supports, a γ-Al_2O_3 interdiffusion barrier was deposited by vacuum assisted dip-coating of a 1.2 wt% boehmite-PVA-PEG solution, rotary drying at 60% relative humidity and 40 °C, and sintering in air atmosphere at 550 °C for 1h, as per our previous works [26].

The supports surface pre-treatment procedure is illustrated in Fig. 1.

All the pre-treatments were characterized for each of the sample supports with the characterization techniques discussed in the next sections.

Finally, membrane M3 was prepared via electroless plating of Pd. The membrane was fabricated onto a support presenting average surface roughness (Ra), average profile heigh (Rz), average in-pore filling (Δ), and average pore diameter (d) below the targets set with this work. The plating bath was composed of Pd(II)Acetate, EDTA, NH_4OH 1 M, and $AgNO_3$, according to the procedure developed in previous works by Tanaka et al. [43]. The modified support was seeded with Pd nuclei in 0.6 vol% Pd(II)Acetate in chloroform and reduced in hydrazine 1 M. Thereafter, the substrate was submerged in the plating bath for 2 h in presence of hydrazine. Subsequently, a 0.113 mmol/L $AgNO_3$ solution was added to the bath with an addition rate of 0.04 ml/min. After 5 h the membrane was removed from the plating bath, thoroughly rinsed with demi water inside and out, and annealed at 550 °C in Ar/H_2 atmosphere for 4 h, with a heating ramp of 1 °C/min in sole Ar.

2.2. Statistical analysis

2.2.1. Sampling

In our previous work [30], a balanced design of in-pore measurements (via laser-confocal microscopy) on a population of support pores using solely 3 supports was proposed as starting point for considerations about the effects of support filler size and amount of filling cycles employed. In this work, the aim is to expand the analyses to a population of different supports, rather than solely different pores. This allows for more precise inference on the effects that each support pre-treatment has on the following one. 20 supports have been prepared and 5 random pores (or positions, in case of contact profilometry) are analyzed, expanding the power of the analysis. The use of different supports allows the measurement of each support's pore diameter distribution (PSD) after each pre-treatment, adding the support's average pore diameter as outcome variable to the analysis.

The use of a sample of 20 prepared supports is considered representative of a population of different supports, each independent from another and each containing a population of pores. The representativeness of the sample is ensured by the randomness of supports choice, which are drawn from supplied 50 cm supports randomly cut and mixed into a batch of 10 cm supports. Meanwhile, the population of pores on each support is analyzed with a sample of 5 observed images (or positions) for each support. The imaging is carried out as randomly as possible, positioning the microscope lens (or the profilometer) onto different locations of the examined support, avoiding selection bias as much as possible. However, due to experimental effort, solely 5 pores and positions are examined for each support. Even though ANOVA is

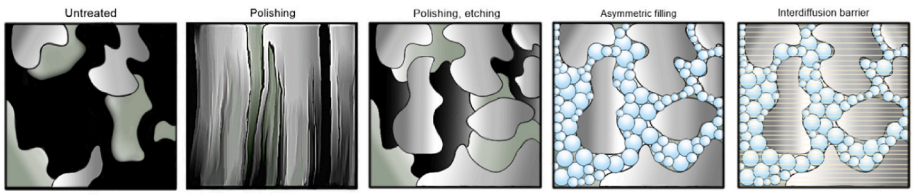

Fig. 1. Illustration of the operated support pre-treatments, support surface view.

considered robust for small sample sizes whether the design is balanced and the data respects variance homogeneity [46–49], the small imaging sample size is to be taken into account during the observation of statistical inference, coupling the results with the observation of descriptive statistics (i.e. density plots, boxplots, average values) or eventual previous analyses (i.e. the inference carried out in our previous works [30]). Even though exploratory, taking into account its limitations, this design opens the possibility for a cohesive analysis of the changes occurring with each support pre-treatment and how these changes may influence the next preparation steps within a whole production population, ultimately giving precious insight on the actual, factual reproducibility of the membrane supports and, in turn, the membranes themselves. Moreover, it represents a starting point for similar, additional statistical studies which can ultimately increase the sampling size, yielding to a greater amount of information and a greater inferential precision.

For this analysis, the seeding and plating procedures have been excluded from the evaluation, as they do not represent critical reproducibility steps. Both plating and seeding procedures are in fact optimized for ceramic supports within the targeted surface characteristics and are not expected to fail once a support is properly tuned to the desired performance.

2.2.2. *Outcome variables evaluation: characterization techniques*

For each support modification treatment, the following characterization techniques were employed.

1. The pore morphology was analyzed via laser-confocal microscopy (Laser-optical confocal microscope, Keyence, Osaka, Japan) by imaging 5 random pores on each support's surface, yielding to the *outcome variable* Δ, to be intended as the difference between the highest and lowest point of the imaged pore's height distribution (Fig. 2).
2. The supports surface roughness was analyzed via contact profilometry (MarSurf PS 10, Mahr) on 5 random positions of the selected support, yielding to *outcome variables Ra (Avg. surface roughness)* and *Rz (Avg. roughness profile's height),* characteristic roughness profile parameters.
3. The pore size distribution of the supports was measured via Capillary Flow Porometry (CFP) in a specifically designed setup described in our previous work [30]. The *average pore diameter (Mean flow pore)* was kept as outcome variable.

2.2.3. *Design of experiment (DoE)*

The analysis proposed in this work was carried out for the following treatment stages, with the DoE configuration reported in the supplementary tables to this manuscript.

1. Untreated supports: The sample of untreated supports is considered representative of a population of supports provided by the supplier, as well as supports which might be employed by any membrane preparation operator who intends to reproduce a highly selective Hastelloy X supported Pd-based membrane. For this reason, 14 supports were characterized with the aim to assess the outcome variables variability within each of the supports and between different supports. A One-way ANOVA was then used to compare the outcome variables between supports.
2. Polished and etched supports: The supports were polished and etched according to the methodology described in section 2.1. The design was balanced by adding 6 supports, increasing the sample size to 20. In particular, any statistical changes caused by the treatments were compared with their untreated version. A One-way ANOVA was used to compare the outcome variables between supports.
3. Symmetrically filled supports: each etched and polished support was filled with α-Al_2O_3 of two different sizes (18 μm, 5 μm), for different amounts of times (20x, 30x), with the procedure described in section 2.1. For each filling cycles-filler size combination, 5 repetitions for all outcome variables were carried out. For this analysis, all outcome variables were normalized on their correspondent unfilled values from the previous step. A Two-way ANOVA was then employed to assess whether the variation of either factor (filling size or filling cycles) or their interaction (filling cycles-filler size) generated statistically significant changes in the selected outcome variables.
4. Asymmetrically filled supports: 5 symmetrically filled (18 μm, 30x) supports were selected for asymmetric filling design, based on the results of the previous analyses (discussed in the next sections). The supports were completed by the addition of α-Al_2O_3 particles with average diameter of 5 μm and 1.5 μm, for an amount of 30 cycles per size, as per preparation procedure. Each outcome variable was evaluated, and a One-way ANOVA was performed to assess differences between supports. The results were then compared with previous pre-treatments.
5. Supports equipped with interdiffusion barrier: The 5 supports were completed with the addition of the γ-Al_2O_3 interdiffusion

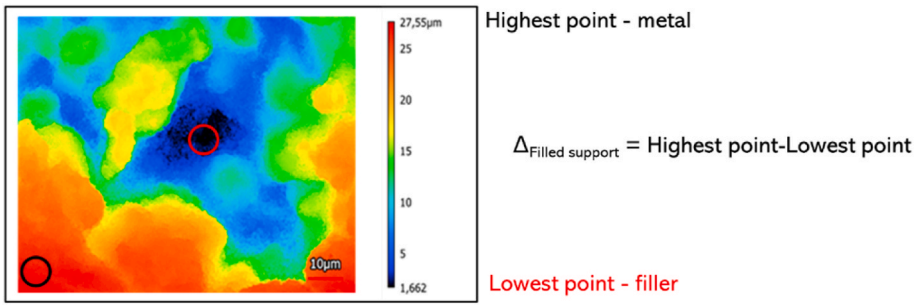

Fig. 2. Laser-confocal imaging, height distribution view and Δ definition.

barrier, which was deposited via vacuum-assisted dip-coating with the constant parameters summarized in section 2.1. Each outcome variable was evaluated once again, and a One-way ANOVA was performed to assess differences between supports. The results were compared with previous pre-treatments.

2.2.4. ANalysis of VAriance (ANOVA)

The two main aims of classical ANOVA [45] are.

1) To examine the relative contribution of different sources of variation (i.e., factors or combination of factors) to the total amount of variation in the response variable (i.e., dependent variable, influenced outcome variable).
2) To test the null hypothesis (H_0), specifically:

H0. The means of the independent groups of observations are not statistically different (p-value >0.05).

H1. There is at least one statistically different mean among the independent groups (p-value <0.05).

Considering the sum of squares (*SS*) and the degrees of freedom (*df*) **between** examined groups (*B*):

$$SS_B = \sum n_k(\overline{Y}_k - \overline{Y})^2 \quad (1)$$

$$df_B = k - 1 \quad (2)$$

And **within** groups (*W*):

$$SS_W = \sum (Y_i - \overline{Y}_k)^2 \quad (3)$$

$$df_W = N - k \quad (4)$$

Where n_k is the number of cases in a sample, $\overline{Y}_k$ the mean of the group, $\overline{Y}$ is the overall mean (grand mean), k is the total number of groups, Y_i is the individual score in a group, and N is the number of observations.

The F-ratio (representing the ratio of between groups variance and within group variance) is then calculated as the ratio between the mean sum of squares between groups and the mean sum of squares within groups:

$$\mathrm{F-ratio} = \frac{SS_B/df_B}{SS_W/df_W} \quad (5)$$

Therefore, the higher the F-ratio the larger the variation between groups of observations rather than the variation within groups of observations. To a larger F-ratio corresponds a lower p-value, which allows for the rejection of the null hypothesis if p-value <0.05.

A One-way ANOVA was used to analyze the means of independent groups of observations for an outcome variable influenced solely by one independent factor (support code).

A Two-Way ANOVA + interaction was used to examine the interaction between two independent variables (filler size and filling cycles). Interactions indicate that differences are not uniform across all levels of the independent variables, meaning the factors cannot be considered independent from each other in their contribution to the variance of the selected outcome variable. The experiment was designed in a balanced way (guaranteeing an equal number of observations for each levels combination).

Each ANOVA analysis relies on three pillar assumptions.

1. The population from which samples are drawn is normally distributed (Normality).
2. The samples are independent and random with respect to each other (Randomness of sampling).
3. The variances among the groups are approximately equal (Homogeneity of variances or Homoskedasticity).

The assumptions for each employed ANOVA were verified for each analysis by observing.

1. The normal probability plot paired with a Shapiro-Wilk test for normality [50]; whether the data did not assume a normal distribution, a Log transform or Sqrt transform were performed on the dataset, according to the skewness of the data distribution.
2. Residuals vs order plot for randomness of sampling.
3. Residual vs fit plot paired with a Levene test for homogeneity of variances [51].

The null hypothesis for ANOVA was accepted if p-value >0.05. A Tukey pairwise comparison was employed as post-hoc test. All analyses were carried out with R language, and the chosen environment was Rstudio [52].

3. Results and discussion

3.1. Characterization of support pre-treatments

Filter E14 was selected from the support's batch for illustrative purposes, while the same analysis was carried out for all supports. In Fig. 3 the surface evolution of filter E14 undergoing the selected pre-treatments is shown in 3D view. In Fig. 3a the untreated support's surface is imaged. Specifically, a large superficial pothole with superficial diameter ~45 μm is noticeable on the untreated support's surface, as well as high profile peaks and deep valleys. In Fig. 3b the surface of the support after polishing and etching is shown. After polishing, the high-profile peaks are lowered, and the surface is leveled. However, porous structures are covered by plastic deformation of the peaks being pushed into the profile valleys, reducing the gas permeation through the support. The porous structure under the polished layer is then uncovered via chemical etching, which results in valley veins interconnecting larger superficial potholes and surrounding the smoothened superficial islands, as shown in the 3D view. These veins contribute to the re-increase of the gas permeance through the support. In Fig. 3c the 3D view of a support's large pothole both empty and filled with α-Al_2O_3 of decreasing size is shown. 18 μm α-Al_2O_3 is layered first with the aim of clogging the large pore necks and reducing the support's average pore size. 5 μm and 1.5 μm α-Al_2O_3 are then subsequently layered to improve the leveling of the pore mouth. In this way, the asymmetrical filler operates a progressive closure of the pothole, reducing its average diameter. In Fig. 4 the reduction in average pore diameter of the support E14 is monitored by analyzing the pore flow distribution of the support after each pre-treatment via CFP coupled with height distribution by laser-optical imaging analysis. When the support is solely polished and etched it presents large pore mouths (blue) interconnected by valley veins (green), with a large height difference and an average pore diameter of ~1.5 μm (Fig. 4a). When the support is asymmetrically filled, the closure and leveling effect on the pore mouth is observed with the shift of the height distribution, the presence of the filler in the pore mouth (green) and the average pore diameter shift to ~ 500 nm (Fig. 4b). After the addition of the interdiffusion barrier, the leveling effect is even more pronounced in the height distribution view, where a layer covering the pore mouth (green), reducing the pore valleys size (red), and pushing the average pore diameter below 100 nm can be clearly distinguished Fig. 4c. Deposition of Pd via seeding-electroless plating procedure on supports pre-treated following the same techniques resulted in highly H_2 selective membranes (ideal H_2/N_2 selectivity >10 000) employed in our previous works [13,30,53] and summarized in Table 1.

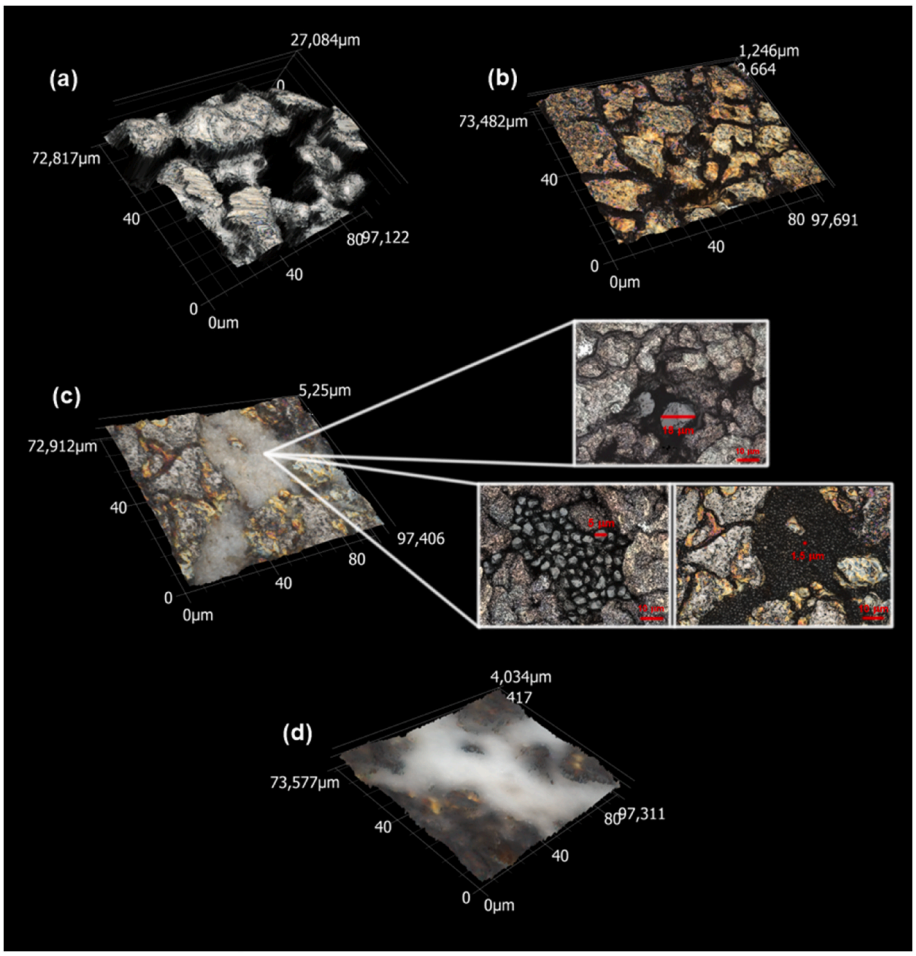

Fig. 3. 3D Laser-optical imaging of (a) Untreated E14 support's surface. (b) Polished, etched E14 support's surface. (c) E14 support's surface asymmetrically filled with α-Al_2O_3 18 µm, 5 µm and 1.5 µm, each imaged in surface view. (d) E14 support's surface equipped with γ-Al_2O_3 interdiffusion barrier.

3.2. Statistical analysis of support pre-treatments

3.2.1. Untreated supports

Fig. 5 reports the boxplot representation of in-pore morphology (Δ), average surface roughness (Ra), and average profile height (Rz) of completely untreated supports. The length of the box and the whiskers for each sample denote a large variability within the repetitions for each support, meaning that the examined variables can significantly change with respect to the randomly chosen measured pore/position. The average values of the outcome variables correspond to Δ = 26.9 µm, Ra = 4.3 µm, Rz = 25 µm. These values of surface roughness are well in agreement with bare PSS substrates previously investigated in literature for the preparation of metallic supported Pd-based membranes. In particular, high surface roughness and large pore mouths have been observed via SEM imaging in several membrane preparation studies, for Porous Stainless Steel (PSS) and Hastelloy X [25] supports ranging between 0.1 µm and 0.5 µm media grade both in tubular and disk form [42, 54–57]. Ryi et al. [58] utilized 3D renders of acquired 0.5 µm PSS substrates and evaluated their height distribution, observing a height difference (similarly to the Δ variable analyzed in this work) of ~10 µm. Such height difference, associated with high surface roughness (topographically observed or measured via contact profilometry/atomic force microscopy/laser-optical microscopy, etc.) is thought to impede the deposition of defect-free Pd thin films, requiring support modification steps to achieve acceptable support's surface characteristics.

The results of the One-way ANOVA between supports for each outcome variable are reported in Table 2. The average values of Δ and Rz are not statistically different in a significant way between each of the prepared sample supports. This result denotes how at this stage, right after the supports are supplied, cut, and welded, each of them can be considered quite similar to one another. The morphological characteristics of each filter are variable within each one of them, but if they are compared to one another, they do not significantly differ. The only variable that presented a significant difference corresponds to Ra. By applying the Tukey pairwise comparison, each pair of average Ra between supports are compared, allowing to understand which sample supports present Ra that are statistically different from each other. In the selected supports batch, the Tukey pairwise comparison highlighted a statistical difference solely between average Ra of sample D and sample F. This result allows to speculate that, if the examined support batch is representative of a population of supplied supports, at least 2 in 20 supplied samples might significantly differ from each other in terms of average surface roughness.

3.2.2. Polished and etched supports

Once physico-chemical support pre-treatments are operated, a variability increase within the dataset can be noticed in terms of visual differences between each filter, as large numbers of boxes fall outside of each other for each outcome variable (Fig. 6)

The results of the One-way ANOVA on each outcome variable are reported in Table 3. A very strong statistically significant difference is confirmed between each support for all the examined outcome parameters. The Tukey pairwise comparison highlights differences between 4 pairs of supports with respect to Δ, 43 with respect to Ra, and 27 with respect to Rz. These results highlight the random effect of the operated physico-chemical pre-treatments: even though the initial batch is of non-

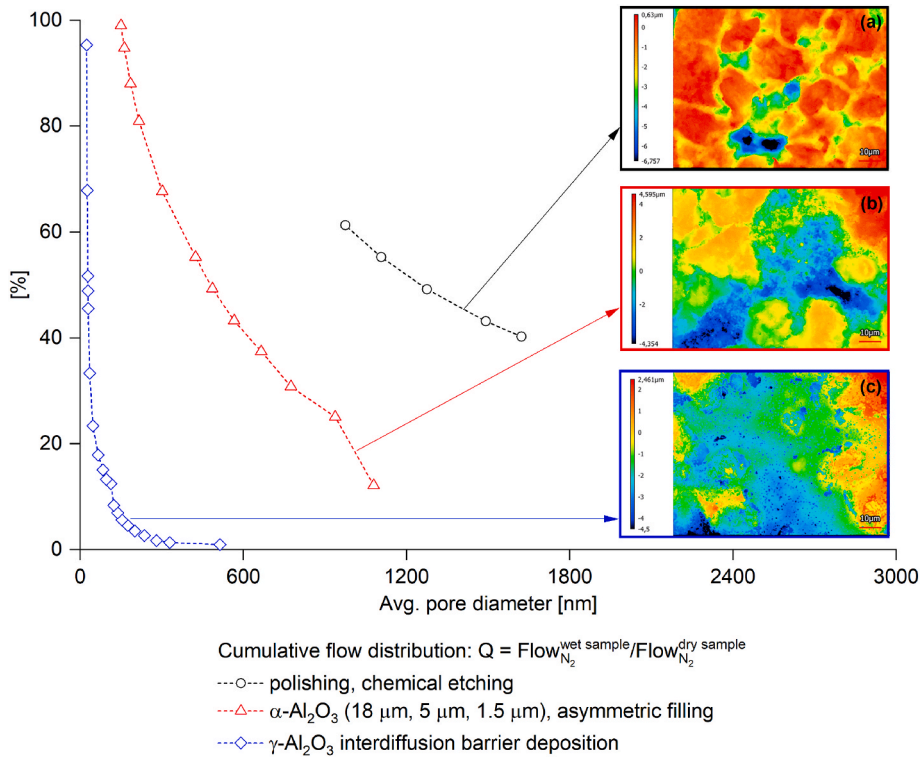

Fig. 4. Pore flow distribution and height distribution view of (a) polished and etched E14 support. (b) E14 support asymmetrically filled with α-Al_2O_3 18 μm, 5 μm and 1.5 μm. (c) E14 support equipped with a γ-Al_2O_3 interdiffusion barrier.

Table 1
Average Pd–Ag layer thickness, H_2/N_2 selectivity, H_2 permeance, and N_2 permeance (evaluated at a temperature of 500 °C and 1 bar *trans*-membrane pressure) of composite Hastelloy X/α-Al_2O_3/γ-Al_2O_3/Pd–Ag membranes presented in our previous works.

Membrane	Average Pd–Ag layer thickness [μm]	H_2/N_2 selectivity (500 °C, 1 bar) [−]<	H_2 permeance (500 °C, 1 bar) [mol/s/m^2/Pa]	N_2 permeance (500 °C, 1 bar) [mol/s/m^2/Pa]	Reference [−]
M0	6–8	53487	~$9.7{\cdot}10^{-7}$	~$1.8{\cdot}10^{-11}$	[30]
M1	6–8	38839	~$7.3{\cdot}10^{-7}$	~$1.9{\cdot}10^{-11}$	[13]
M2	6–8	20270	~$7.5{\cdot}10^{-7}$	~$3.7{\cdot}10^{-11}$	[53]

statistically different supports, the pre-treatments increase the morphological differences between each filter. These differences imply an intrinsic difficulty in controlling the process around a desired average value for all the observed outcome parameters, particularly in terms of average surface roughness, with the highest observed number of statistically different support pairs. This increased difference between supports proves inconvenient in terms of reproducibility, as these differences can propagate to the following filling procedure.

In Fig. 7, the data distributions for each outcome variable before and after the physico-chemical pre-treatments are compared. A shift towards lower Δ, Ra and Rz values can be observed, with average Δ = 19.62 μm, Ra = 1.28 μm, Rz = 10.35 μm. This confirms the effectiveness of the chosen treatments in terms of shift of morphological characteristics towards a smoother, more even surface. Moreover, in Fig. 7a a higher distribution spread with respect to the untreated supports morphological data distribution for Δ can be observed. This behavior indicates the introduction of morphological differences within the in-pore behavior of the support itself, as the randomly chosen measurement points yield to more variable results after the pre-treatments. This might suggest that, at this stage, the distance between pore valleys and superficial peaks is quite variable along each support. In Fig. 7b and c little variation of the distribution spread is observed, indicating that the variability of Ra and Rz stays the same after the support physic-chemical pre-treatments, denoting a variable surface roughness profile but an overall smoother surface.

In several literature works, as-supplied PSS and Hastelloy X supports are treated via surface polishing in order to reduce their original surface roughness. Generally, all the examined literature works confirm the effectiveness of this pre-treatment by observing morphological surface changes via SEM imaging of a treated sample [25–27,55,59,60]. The proposed analysis of a larger batch of supports and the observation of the surface roughness variables evolution within the batch confirmed the average smoothening effect of this strategy but highlighted its random nature, emphasizing the need for a quality check on each support, on different points of the surface.

3.2.3. *Symmetrically filled supports*

For the optimization of the filling procedure, it is crucial to understand the morphological changes that occur when fillers of different sizes are applied to the chosen supports. In the work of Macedo et al. [22], several dimensions of Ceria particles have been evaluated to find the most appropriate size for membrane interlayer fabrication. Similarly, Xu et al. [27] coated a PSS substrate with alumina powder of different particle size suspended in water. In our previous work [30], the morphology of three different supports consecutively filled with alumina 18 μm, 5 μm, and 1.5 μm for an increasing number of times (10x, 15x, 20x) was studied by proposing the classical observational method coupled with a preliminary statistical investigation. The ANOVA then allowed to infer on a population of pores of three supports. It was then assumed that the three supports behavior could be applied to

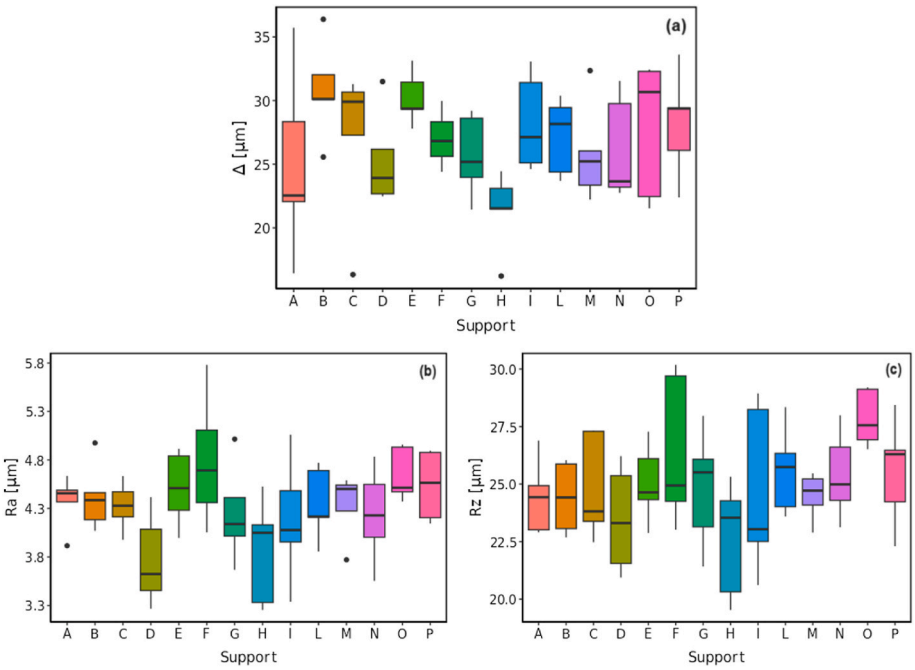

Fig. 5. Boxplot of (a) Δ, (b) Ra, (c) Rz for each untreated support of the chosen sample batch.

Table 2
Results of One-way ANOVA on Δ, Ra, Rz of fully untreated supports.

In-pore morphology, Δ [μm]			
Factor	F-value	P-value	Significance
Support code	1.503	0.145	no
Avg. Profile surface roughness, Ra [μm]			
Factor	F-value	P-value	Significance
Support code	1.919	0.047	*
Avg. Profile height, Rz [μm]			
Factor	F-value	P-value	Significance
Support code	1.525	0.137	no

Tukey pairwise comparison: D-F.

different supports from different batches of the same supplier. While this speculation can be considered reasonable as hypothesis, it would still be unverified by objective experimental data, unless more modified supports are prepared with the same procedure as the considered three supports. In the case of membrane M2 of our SMR work [53], a target of support reproducibility was derived from the analysis carried out in Ref. [30]. However, to be able to confirm that the behavior of the filler particles is actually extendible to a population of supports, the analysis must be expanded on pores coming from a representative support sample. For this purpose, the results of the extended Two-way ANOVA are listed in Table 4.

The Two-way ANOVA results for the reduction of Δ confirm the in-pore behavior observed in our previous work [30]: as the interaction contribution is statistically significant, it is not possible to decouple the effects of solely filling cycles or filler size on the observed supports. A 5 μm filler improves the superficial morphology of the supports with less filling cycles with respect to the filler of larger size, which requires a larger number of cycles (Fig. 8a). However, when the analysis is extended to a batch of supports there is no detectable statistical difference between the average values of Ra and Rz between supports filled in different ways. These findings indicate that, the selected filler sizes and cycle count do not exhibit a noticeable impact on the surface roughness

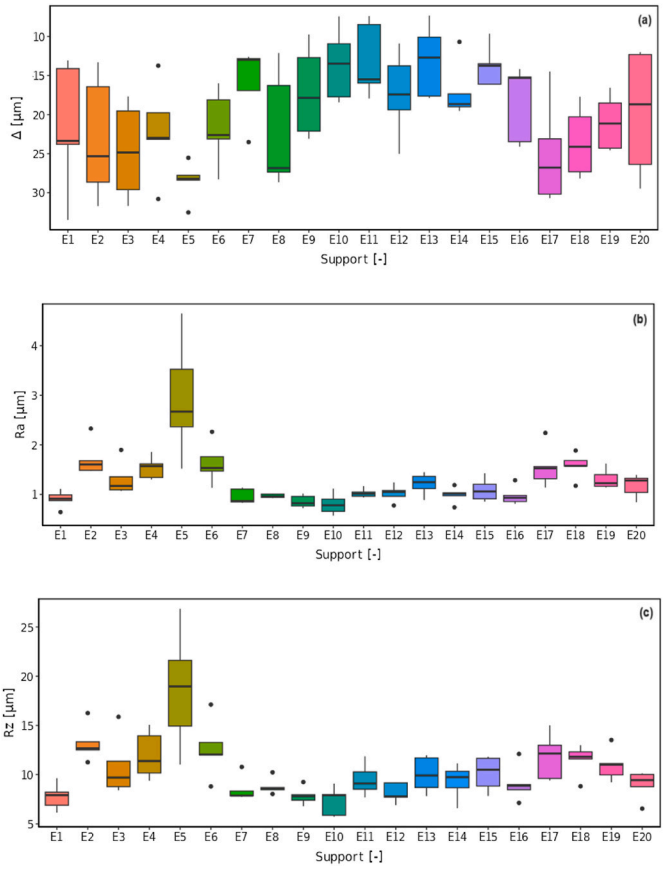

Fig. 6. Boxplot representation of (a) Δ, (b) Ra, (c) Rz for each filter of the sample batch after polishing and etching pre-treatments.

parameters of the profile. Rather, their influence appears to be confined solely to the behavior within the pores. However, the acceptance of ANOVA's null hypothesis for outcome variables Ra and Rz could also be

Table 3
Results of One-way ANOVA on Δ, Ra, Rz of polished and etched supports.

In-pore morphology, Δ [μm]			
Factor	F-value	P-value	Significance
Support code	3.11	$2.11 \cdot 10^{-4}$	***
Avg. Profile surface roughness, Ra [μm]			
Factor	F-value	P-value	Significance
Support code	9.05	$4.15 \cdot 10^{-13}$	***
Avg. Profile height, Rz [μm]			
Factor	F-value	P-value	Significance
Support code	5.98	$5.02 \cdot 10^{-9}$	***

Tukey pairwise comparison: 4 statistically different pairs.
Tukey pairwise comparison: 43 statistically different pairs.
Tukey pairwise comparison: 25 statistically different pairs.

reconducted to a Type II error (wrongly accepting a null hypothesis), due to the combined effect of high variability of the surface profilometry data and the small sample size for each support. In our previous analysis, in fact, the examined filler sizes and filling cycles sorted an effect on profile roughness parameters when a larger sample of pores (on solely 3 supports) was observed [30].

This conclusion suggests that.

1) the expansion of the analysis to a larger sample of support pores (e.g. 30 repetitions for each support), although time-consuming, would exclude the possibility of neglecting statistically significant differences between outcome profile roughness parameters, which are intrinsically more variable.
2) if Type II error may be excluded, to sort a sensible effect also on profile roughness parameters, the analysis should be expanded to different filler cycles-filler size combinations. More specifically, as fillers of 5 μm seem to sort the greatest effect on in-pore leveling, their combination with a larger number of filling cycles (i.e., 50x, 60x) could be explored, and the effect on profile roughness parameters assessed. Moreover, filler particles between 5 and 18 μm (i.e. ~ 10 μm, 8 μm) could be added to the analysis, allowing to select an optimized combination and to infer on a greater plethora of possibilities to find an optimum filler.

Concerning the average pore diameter of the support, the results in Table 4 confirm that even for a population of supports, the size of the filler is the dominating factor (main and sole statistically significant effect) that will promote a reduction in the average pore diameter. Similarly, in Ref. [22], the supports prepared with an interlayer particle size best matching the diameter of the chosen PSS substrate (medium Ceria particles – 0.1 μm media grade PSS) led to the highest H_2 permeance and the best observed surface morphology amongst the presented samples, suggesting an effect of the filler size on a sensitive variable, which was identified in this work as the average pore diameter of the supports.

As observed in Fig. 8b, the 18 μm filler promotes a statistically significant decrease in average pore diameter with respect to the smaller filler, completing the purely observational results reported in Ref. [30] with statistical meaning.

Given these results, and critically accounting for their limitations, the development of an asymmetrical filling configuration is backed up by mathematical considerations on the gathered datasets. In particular.

1. The variability increase given by the polishing and etching pretreatments needs to be resolved by the following filling design and/or interdiffusion barrier deposition.
2. Fillers of largest size promote a statistically significant decrease in the average pore diameter of the supports.
3. Fillers of largest size require a larger number of cycles to operate in-pore morphological changes, while fillers of smaller sizes can require less.

Asymmetrically filled supports

Given the considerations in the previous analysis, five supports filled with 18 μm α-Al_2O_3 particles were chosen as starting point for the asymmetrical filling evaluation. They were then completed with 5 μm and 1.5 μm particles and analyzed as is. The results of the One-way

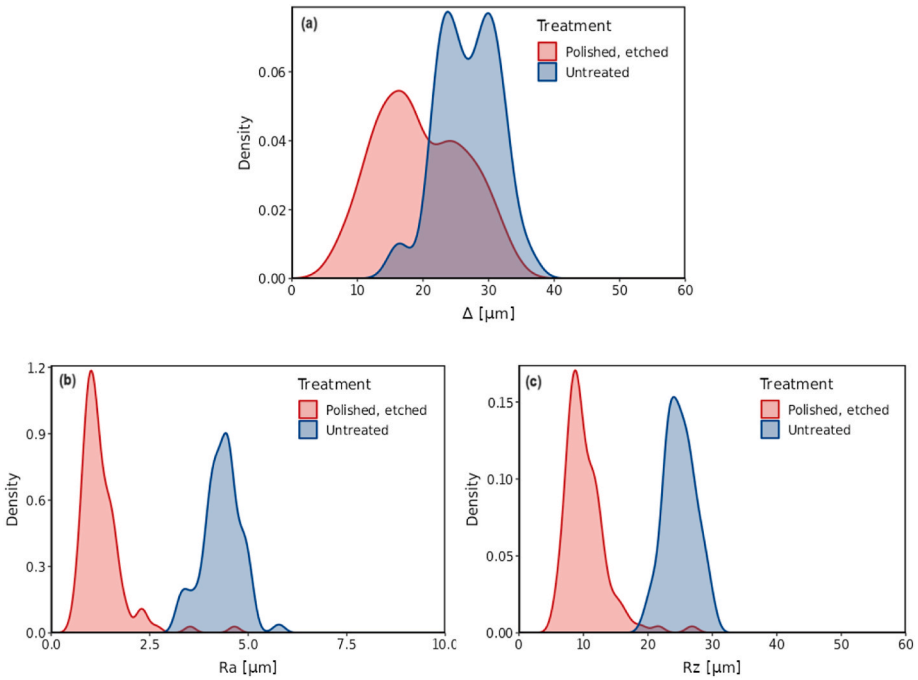

Fig. 7. Comparison of density plots of (a) Δ, (b) Ra and (c) Rz between the sample batch of polished and etched supports (red), and the sample batch of fully untreated supports (blue). (For interpretation of the references to colour in this figure legend, the reader is referred to the Web version of this article.)

Table 4
Two-way ANOVA + interaction results for Δ reduction, Ra reduction, Rz reduction and average pore diameter reduction promoted by the factors filler size and filling cycles.

In-pore morphology, $\Delta_{reduction}$ [%]			
Factor	F-value	P-value	Significance
Filler size	2.67	0.11	No
Filling cycles	0.51	0.48	No
Filler size:Filling cycles	13.54	0.0004	***
Avg. Profile surface roughness, $Ra_{reduction}$ [%]			
Factor	F-value	P-value	Significance
Filler size	1.03	0.31	No
Filling cycles	2.23	0.14	No
Filler size:Filling cycles	1.36	0.25	No
Avg. Profile height, $Rz_{reduction}$ [%]			
Factor	F-value	P-value	Significance
Filler size	0.02	0.88	No
Filling cycles	1.96	0.16	No
Filler size:Filling cycles	2.63	0.11	No
Avg. Pore diameter reduction [%]			
Factor	F-value	P-value	Significance
Filling cycles	2.28	0.17	No
Filler size	6.55	0.03	*
Filler size:Filling cycles	0.82	0.39	No

ANOVA are listed in Table 5. By analyzing the effect on Δ of the asymmetric filling design, no statistically significant differences between the selected supports are detected. This result proves that the chosen asymmetric filling design reduces the differences between in-pore behavior of different supports, eliminating the differentiating effect sorted by the polishing and etching treatment. In Fig. 9a, all the Δ distributions for the examined supports overlap around a similar average value, while their spreads still differ from each other. This result denotes quite some variability within the pores of the supports themselves. Specifically support E1, given the larger spread of its morphological distribution. At this stage, the variability within the pores of filled supports is inevitable, but such a spread for an isolated sample could be due to the intrinsic difficulty in controlling the filling procedure in the laboratory. Hence why the fabrication, monitoring and characterization of twin supports is so crucial to ensure membrane repeatability. Particularly, given the spread of its in-pore characteristics, E1 support has a higher chance of resulting in a membrane with defects, making it harder to control its pore closure.

Concerning the outcome variables Ra and Rz, the ANOVA results highlight statistical differences. Specifically, support E14 presents a strongly different Ra with respect to the others, while Rz differs generally for supports E14 and E12. These results indicate once more the difficulty in controlling profile surface roughness parameters solely by introducing a pore filler in the support. In Fig. 9b and c, the differences between the distributions can be distinguished in the density plots, where E14 is clearly shifted towards the left, differentiating its average value from the other supports.

In Fig. 10, a clear distribution shift towards lower average pore diameters after the introduction of the asymmetric filler is observed. However, the distribution spread increases, meaning that after filling the average pore diameter is quite different amongst different supports. At this stage, it is important to properly design the amount of filling cycles to reach a target pore size, as demonstrated in our previous work for steam methane reforming [53]. In our previous work, we chose 100 nm as target to be as close as possible to a ceramic support average pore diameter. In this batch, the target is reached by the supports falling within the distribution's left tail. However, in the case of the right distribution tail (average pore diameter's distribution peak ~ 500 nm), the filling should be carried out once more to reach the target and ensure high selectivity on the final membrane.

3.2.4. *Supports equipped with interdiffusion barrier*

In Table 6, the results of the performed One-way ANOVA after interdiffusion barrier deposition are reported. All statistical differences between the supports have been erased by the deposition of the layer, except for the outcome variable Rz. However, the Tukey pairwise comparison detected a difference only between two supports, E1 and E12. The differences between supports E1 and E12 in terms of Rz can be explained by the nature of Rz variable, which detects all possible peaks and valleys of the measured profile, retaining more information about the variability of the profile itself. However, the elimination of most statistical differences for all outcome variables highlights how the interdiffusion barrier deposition promotes the uniformity of all morphological characteristics between different supports. This behavior is shown in Fig. 11, where the density plots for the outcome variables are compared amongst the supports of the batch. Particularly, all the

Table 5
Results of One-way ANOVA on Δ, Ra, Rz of asymmetrically filled supports.

In-pore morphology, Δ [μm]			
Factor	F-value	P-value	Significance
Support code	0.84	0.70	No
Avg. Profile surface roughness, Ra [μm]			
Factor	F-value	P-value	Significance
Support code	15.49	$6.39 \cdot 10^{-6}$	***
Avg. Profile height, Rz [μm]			
Factor	F-value	P-value	Significance
Support code	10.64	$8.7 \cdot 10^{-5}$	***

Tukey pairwise comparison: E14-E1, E12-E18, E12-E3, E12-E14.

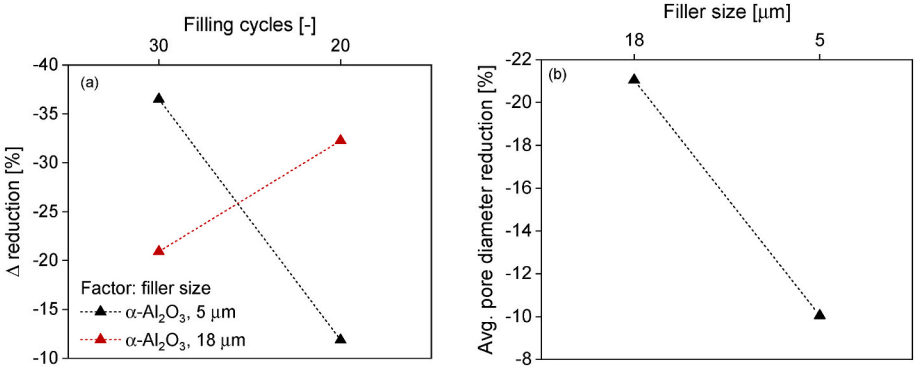

Fig. 8. (a) Interaction plot of Δ reduction for the factors filler size and filling cycles. (b) Main effect plot of average pore diameter reduction for the factor filler size.

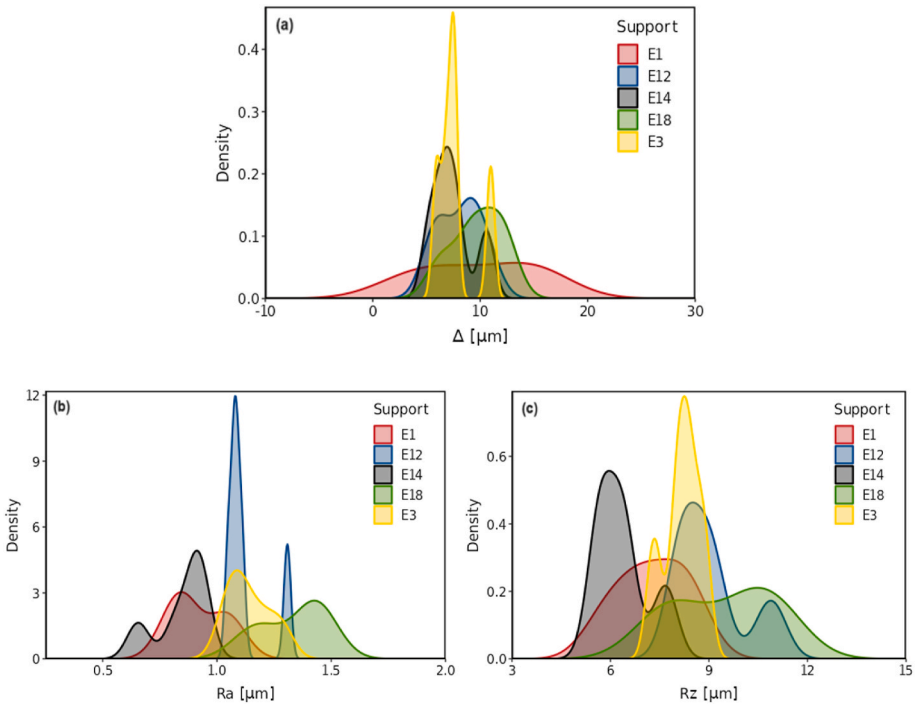

Fig. 9. Density plot of (a) Δ, (b) Ra, and (c) Rz for each asymmetrically filled support.

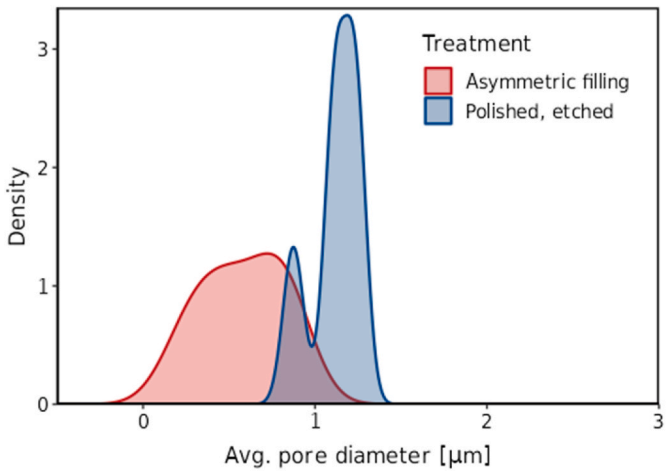

Fig. 10. Average pore diameter density plot evolution. Comparison between solely polished and etched supports and asymmetrically filled supports.

Table 6
Results of One-way ANOVA on Δ, Ra, Rz of supports equipped with interdiffusion barrier.

In-pore morphology, Δ [μm]			
Factor	F-value	P-value	Significance
Support code	2.41	0.09	No
Avg. Profile surface roughness, Ra [μm]			
Factor	F-value	P-value	Significance
Support code	2.15	0.11	No
Avg. Profile height, Rz [μm]			
Factor	F-value	P-value	Significance
Support code Tukey pairwise comparison: E8-E12	3.88	0.0173	*

distributions overlap over the same average values of Δ = 6.88 μm, Ra = 0.814 μm, Rz = 5.77 μm. Even though for some supports (E1, E18, E14) the Δ distribution is still variable, the average value of Δ is sensibly lower if compared to the previous treatment steps. The same behavior is shown in the density plots for macroscopical roughness parameters Ra and Rz (Fig. 11b and c), where the distributions sharpened around lower values.

This data is well in agreement with our previous work [26], in which the smoothening effect of the boehmite based interdiffusion barrier (dual function of preventing strong Pd-support interaction and reducing the surface roughness of the support) was introduced. It is thus possible to confirm the leveling effect of the barrier thanks to the statistical analysis of the selected support batch, considering the interdiffusion barrier as powerful tool to promote uniformity of the morphological characteristics of different supports. Similarly, in previous composite PSS/interlayer/Pd membrane preparation studies presenting different layers as strategy to prevent interdiffusion and improve superficial morphology of PSS/steel-based alloys, the deposition of an intermediate barrier promoted overall surface morphology improvement, pore mouths diameter reduction and general fullness of the PSS substrates, observed mostly via SEM imaging [22,24,28,60–63].

In Fig. 12, the average pore diameter density plot after the introduction of the interdiffusion barrier is shown. It is quite evident how the additional layer sharpens the density plot towards lower average pore diameter values (<500 nm). Particularly, 4 out of 5 of the supports reach the pore size distribution target (<100 nm) after interdiffusion barrier deposition. This result introduces a further effect of the addition of the interdiffusion barrier: even if the asymmetrical filler design leads to pores larger than 100 nm (~500 nm), the introduction of the additional layer will sharpen the average pore diameter below 300 nm for at least half of the examined supports. Therefore, in view of reproducibility, even if the asymmetric filling design is defective, part of the support batch can be recovered by means of addition of the interdiffusion barrier.

3.2.5. *Reproducibility considerations*

The results of the ANOVA highlighted.

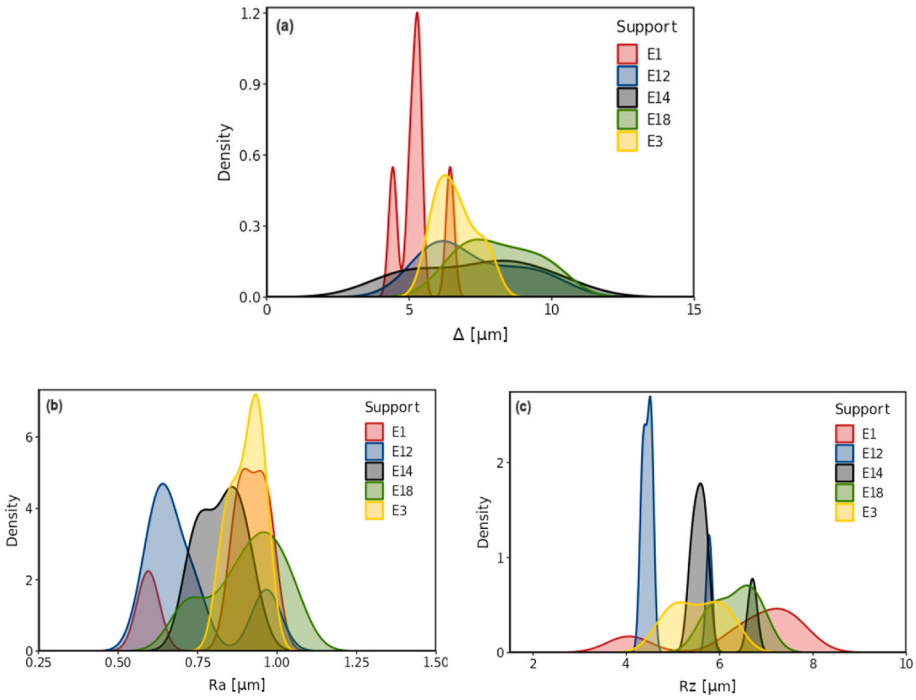

Fig. 11. Density plot of Δ, Ra and Rz for each support of the sample batch of supports completed with the γ-Al_2O_3 interdiffusion barrier.

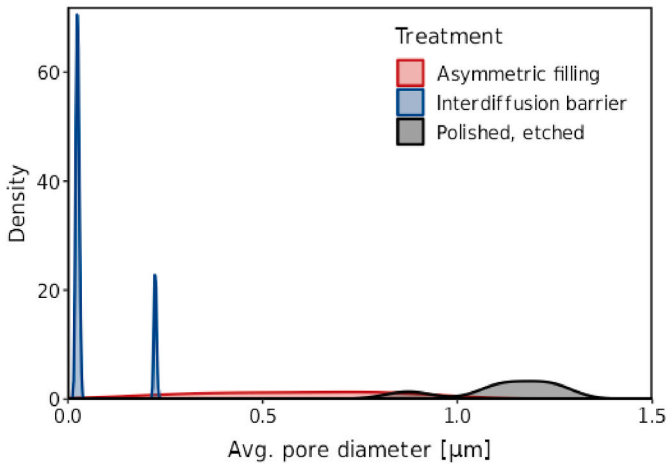

Fig. 12. Average pore diameter density plot evolution. Comparison between solely polished and etched supports, asymmetrically filled supports, and supports equipped with interdiffusion barrier.

1. Negligible statistical difference between morphological variables of untreated supports.
2. Increased statistical difference between polished and etched supports, while promoting surface uniformity.
3. Statistically significant increase in superficial pore leveling operated by 5 μm fillers.
4. Statistically significant reduction in average pore diameter operated by 18 μm fillers.
5. Statistically significant increase in pore leveling operated by asymmetric filling, with negligible statistical differences between in-pore behavior of supports filled in the same way.
6. Statistically significant smoothening effect of γ-Al_2O_3 interdiffusion barrier.
7. Statistically significant reduction in average pore diameter with the introduction of the interdiffusion barrier.

The results confirm the effectiveness of support pre-treatments in smoothening the surface, leveling the pores, and reducing the support's pore diameter; however, they denote variability between the supports and within their profile roughness parameters, highlighting the importance of support's monitoring during the manufacturing process. Suitable targets for support reproducibility are drawn from the analysis of the peaks of density distributions (avg. values), compared with the supports used for best performing membranes (Table 1) as

- Ra < 0.8 μm.
- Rz < 7 μm.
- Average pore diameter after asymmetric filling ~100–500 nm (with the most effective particle size for pore diameter reduction ~18 μm).
- Average pore diameter after interdiffusion barrier deposition ~100 nm.
- Δ < 6 μm (with the most effective particle size for in-pore leveling $\leq$ 5 μm).

Finally, the performance indicators and support characteristics of M3, fabricated on a support with the proposed targets, are shown in Table 7.

This membrane displays selectivity >10000 and H_2 permeance of $6.1 \cdot 10^{-7}$ mol/s/m^2/Pa at 500 °C and 1 bar, similarly to the membranes summarized in Table 1. The high selectivity is promoted by the filling of the metallic support below the proposed targets, which ensure sufficient pore diameter reduction to promote full pore closure with Pd electroless deposition, at constant Pd–Ag thickness. On the other hand, the filling of the metallic support and the deposition of the interdiffusion barrier result in H_2 permeance values which are lower compared to Pd-based membranes obtained on ceramic supports (i.e. Arratibel et al. [64] could produce α-Al_2O_3/Pd–Ag/γ-Al_2O_3 ceramic supported, double skinned membranes which could reach up to $5 \cdot 10^{-6}$ mol/s/m^2/Pa at 500 °C, 1 bar while keeping outstanding H_2 selectivity of 30000). However, for porous metal supports (particularly with media grade $\geq$0.5 μm), the closure of the large superficial pores via introduction of a filler and/or the deposition of an interdiffusion barrier are crucial, unavoidable steps to ensure gas tightness of the metallic supported Pd membrane and prevent Pd-metal interaction. Their presence in the

Table 7
M3 support characteristic variables (Δ, Ra, Rz, and avg. pore diameter) compared with the proposed support targets and resulting membrane performance after Pd–Ag deposition in terms of: H_2 permeance, N_2, permeance, ideal H_2/N_2 selectivity measured at 500 °C and 1 bar *trans*-membrane pressure.

SUPPORT			MEMBRANE	
M3 support (Hastelloy X polished, etched/ α-Al_2O_3/γ-Al_2O_3)		Target	M3 membrane (Hastelloy X polished, etched/ α-Al_2O_3/γ-Al_2O_3/Pd–Ag)	
Ra [μm]	0.782	<0.8	**Pd–Ag layer thickness [μm]**	6–8
Rz [μm]	5.790	<7.0	**H_2 permeance [mol/s/m^2/Pa]**	~$6.1{\cdot}10^{-7}$
Δ [μm]	5.115	<6.0	**N_2 permeance [mol/s/m^2/Pa]**	~$2.4{\cdot}10^{-11}$
d [μm]	0.069	~0.100	**H_2/N_2 selectivity [−]**	25416

support structure and their design was shown to significantly impact membrane's H_2 permeation [65–67].

The characteristic exponent of M3 was retrieved via linear fit of the H_2 permeating flux across the membrane at 400, 450 and 500 °C (Fig. 13) and amounts to $n = 0.5$ with a $R^2 = 0.99$. Moreover, the membrane's activation energy amounts to $Ea = 9.6$ kJ/mol, well in agreement with values of activation energy for metallic supported Pd-based membranes [25,60].

By fabricating M3, the proposed support preparation procedure resulted once again in a highly selective membrane (at constant Pd–Ag layer thickness). However, to fully confirm a statistical (and not solely observational) correlation between the Pd layer performance in terms of H_2 permeance and H_2/N_2 selectivity and the support variables Δ, Ra, Rz, and d further DoE studies with an increased number of membrane repetitions must be carried out. To reproduce the supports proposed in this work, the analysis suggests the adoption of the proposed targets for the modification of PSS/steel alloy supports with similar superficial characteristics, rather than a set-in-stone fabrication procedure.

4. Conclusions

Twenty Hastelloy X porous supports, drawn from a supplied supports population, were successfully pre-treated to increase their suitability for Pd deposition via electroless plating. The operated pre-treatments were polishing, etching, symmetric and asymmetric filling with α-Al_2O_3 particles (18 μm, 5 μm, 1.5 μm) and γ-Al_2O_3 interdiffusion barrier deposition. Each pre-treatment step was thoroughly characterized to elucidate the supports' surface evolution.

A Design of Experiment coupled with ANalysis Of VAriance as statistical analysis tool was successfully applied to infer on the morphological effects operated by each pre-treatment on the chosen filter's population.

Suitable targets for supports reproducibility were drawn from the analysis and its comparison with best performing membranes as: Ra < 0.8 μm, Rz < 7 μm, average pore diameter after asymmetric filling ~100–500 nm (most effective particle size for reduction ~18 μm), average pore diameter after interdiffusion barrier deposition ~100 nm, and in-pore leveling (Δ) < 6 μm (most effective particle size for leveling ≤ 5 μm).

These considerations offered further insight on employment of statistics as tool of analysis for composite inorganic membrane preparation, as well as targets to reproduce supports with suitable superficial characteristics for Pd deposition via electroless plating.

CRediT authorship contribution statement

S. Agnolin: Writing – original draft, Investigation, Formal analysis, Data curation, Conceptualization. **F. Gallucci:** Writing – review & editing, Supervision, Funding acquisition, Conceptualization.

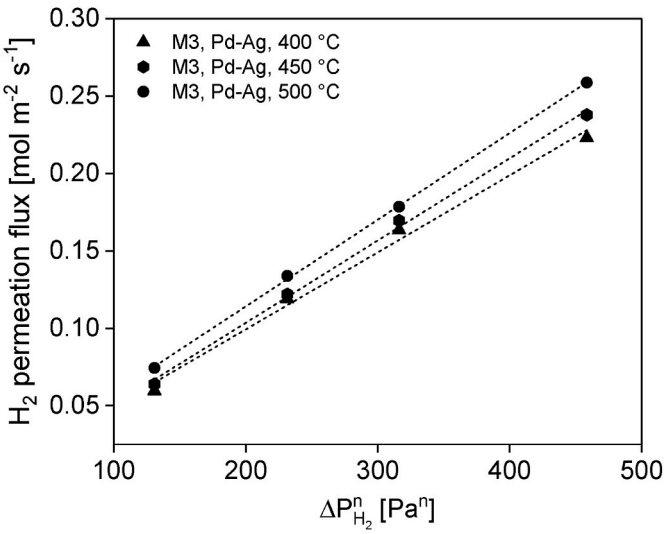

Fig. 13. H_2 permeating flux vs H_2 partial pressure of M3, evaluated at 1, 2, 3, and 5 bar *trans*-membrane pressure and at a temperature of 400, 450, and 500 °C.

Declaration of competing interest

The authors declare that they have no known competing financial interests or personal relationships that could have appeared to influence the work reported in this paper.

Data availability

data will be shared in Zenodo

Acknowledgements

This project has received funding from the European Union's Horizon 2020 Research and Innovation Programme under grant agreement No 869896 (MACBETH).

Appendix A. Supplementary data

Supplementary data to this article can be found online at https://doi.org/10.1016/j.memsci.2024.122690.

References

[1] F. Gallucci, E. Fernandez, P. Corengia, M. van Sint Annaland, Recent advances on membranes and membrane reactors for hydrogen production, Chem. Eng. Sci. 92 (Apr. 2013) 40–66, https://doi.org/10.1016/J.CES.2013.01.008.
[2] G. Bernardo, T. Araújo, T. da Silva Lopes, J. Sousa, A. Mendes, Recent advances in membrane technologies for hydrogen purification, Int. J. Hydrogen Energy 45 (12) (Mar. 2020) 7313–7338, https://doi.org/10.1016/J.IJHYDENE.2019.06.162.
[3] E. Fernandez, et al., Palladium based membranes and membrane reactors for hydrogen production and purification: an overview of research activities at Tecnalia and TU/e, Int. J. Hydrogen Energy 42 (19) (May 2017) 13763–13776, https://doi.org/10.1016/J.IJHYDENE.2017.03.067.
[4] F. Gallucci, L. Paturzo, A. Basile, A simulation study of the steam reforming of methane in a dense tubular membrane reactor, Int. J. Hydrogen Energy 29 (6) (2004) 611–617, https://doi.org/10.1016/j.ijhydene.2003.08.003.
[5] C.S. Patil, M. van Sint Annaland, J.A.M. Kuipers, Fluidised bed membrane reactor for ultrapure hydrogen production via methane steam reforming: experimental demonstration and model validation, Chem. Eng. Sci. 62 (11) (2007) 2989–3007, https://doi.org/10.1016/j.ces.2007.02.022.
[6] P. Bernardo, G. Barbieri, E. Drioli, Evaluation of membrane reactor with hydrogen-selective membrane in methane steam reforming, Chem. Eng. Sci. 65 (3) (Feb. 2010) 1159–1166, https://doi.org/10.1016/J.CES.2009.09.071.
[7] A. Arratibel, D.A. Pacheco Tanaka, T.J.A. Slater, T.L. Burnett, M. van Sint Annaland, F. Gallucci, Unravelling the transport mechanism of pore-filled membranes for hydrogen separation, Sep. Purif. Technol. 203 (April) (2018) 41–47, https://doi.org/10.1016/j.seppur.2018.04.016.

[8] J. Park, T. Bennett, J. Schwarzmann, S.A. Cohen, Permeation of hydrogen through palladium, J. Nucl. Mater. 220–222 (2) (1995) 827–831, https://doi.org/10.1016/0022-3115(94)00591-5.
[9] M.L. Bosko, J.F. Múnera, E.A. Lombardo, L.M. Cornaglia, Dry reforming of methane in membrane reactors using Pd and Pd–Ag composite membranes on a NaA zeolite modified porous stainless steel support, J. Memb. Sci. 364 (1–2) (Nov. 2010) 17–26, https://doi.org/10.1016/J.MEMSCI.2010.07.039.
[10] A. Arratibel, D.A.P. Tanaka, M. van Sint Annaland, F. Gallucci, Membrane reactors for autothermal reforming of methane, methanol, and ethanol, Membr. React. Energy Appl. Basic Chem. Prod. (Jan. 2015) 61–98, https://doi.org/10.1016/B978-1-78242-223-5.00003-0.
[11] V. Cechetto, L. Di Felice, J.A. Medrano, C. Makhloufi, J. Zuniga, F. Gallucci, H2 production via ammonia decomposition in a catalytic membrane reactor, Fuel Process. Technol. 216 (2021) 106772, https://doi.org/10.1016/j.fuproc.2021.106772.
[12] V. Cechetto, L. Di Felice, R. Gutierrez Martinez, A. Arratibel Plazaola, F. Gallucci, Ultra-pure hydrogen production via ammonia decomposition in a catalytic membrane reactor, Int. J. Hydrogen Energy (2022), https://doi.org/10.1016/j.ijhydene.2022.04.240.
[13] V. Cechetto, S. Agnolin, L. Di Felice, A. Pacheco Tanaka, M. Llosa Tanco, F. Gallucci, Metallic supported Pd-Ag membranes for simultaneous ammonia decomposition and H2 separation in a membrane reactor: experimental Proof of Concept, Catalysts 13 (6) (2023), https://doi.org/10.3390/catal13060920.
[14] C. Brencio, L. Di Felice, F. Gallucci, Fluidized bed membrane reactor for the Direct dehydrogenation of propane: Proof of Concept, Membranes 12 (12) (2022), https://doi.org/10.3390/membranes12121211.
[15] W.J.R. Ververs, A. Arratibel Plazaola, L. Di Felice, F. Gallucci, On the applicability of PdAg membranes in propane dehydrogenation processes, Int. J. Hydrogen Energy (Jul. 2023), https://doi.org/10.1016/J.IJHYDENE.2023.06.202.
[16] A. Arratibel, A. Pacheco Tanaka, I. Laso, M. van Sint Annaland, F. Gallucci, Development of Pd-based double-skinned membranes for hydrogen production in fluidized bed membrane reactors, J. Memb. Sci. 550 (Mar. 2018) 536–544, https://doi.org/10.1016/J.MEMSCI.2017.10.064.
[17] J. Melendez, E. Fernandez, F. Gallucci, M. van Sint Annaland, P.L. Arias, D. A. Pacheco Tanaka, Preparation and characterization of ceramic supported ultra-thin (~1 μm) Pd-Ag membranes, J. Memb. Sci. 528 (2017) (2017) 12–23, https://doi.org/10.1016/j.memsci.2017.01.011.
[18] S. Uemiya, T. Matsuda, E. Kikuchi, Hydrogen permeable palladium-silver alloy membrane supported on porous ceramics, J. Memb. Sci. 56 (3) (1991) 315–325, https://doi.org/10.1016/S0376-7388(00)83041-0.
[19] N. de Nooijer, et al., Long-term stability of thin-film Pd-based supported membranes, Processes 7 (2) (2019), https://doi.org/10.3390/pr7020106.
[20] R. Sanz, J.A. Calles, D. Alique, L. Furones, New synthesis method of Pd membranes over tubular PSS supports via ' pore-plating ' for hydrogen separation processes, Int. J. Hydrogen Energy 37 (23) (2012) 18476–18485, https://doi.org/10.1016/j.ijhydene.2012.09.084.
[21] J.A. Medrano, et al., Pd-based metallic supported membranes: high-temperature stability and fluidized bed reactor testing, Int. J. Hydrogen Energy 41 (20) (Jun. 2016) 8706–8718, https://doi.org/10.1016/J.IJHYDENE.2015.10.094.
[22] M. Salomé Macedo, et al., Effect of ceria particle size as intermediate layer for preparation of composite Pd-membranes by electroless pore-plating onto porous stainless-steel supports, Sep. Purif. Technol. 327 (Dec. 2023) 124932, https://doi.org/10.1016/J.SEPPUR.2023.124932.
[23] M.J.H. Van Dal, M.C.L.P. Pleumeekers, A.A. Kodentsov, F.J.J. Van Loo, Intrinsic diffusion and Kirkendall effect in Ni-Pd and Fe-Pd solid solutions, Acta Mater. 48 (2) (2000) 385–396, https://doi.org/10.1016/S1359-6454(99)00375-4.
[24] M.L. Bosko, J.B. Miller, E.A. Lombardo, A.J. Gellman, L.M. Cornaglia, Surface characterization of Pd–Ag composite membranes after annealing at various temperatures, J. Memb. Sci. 369 (1–2) (Mar. 2011) 267–276, https://doi.org/10.1016/J.MEMSCI.2010.12.006.
[25] E. Fernandez, et al., Preparation and characterization of metallic supported thin Pd–Ag membranes for hydrogen separation, Chem. Eng. J. 305 (Dec. 2016) 182–190, https://doi.org/10.1016/J.CEJ.2015.09.119.
[26] S. Agnolin, J. Melendez, L. Di Felice, F. Gallucci, Surface roughness improvement of Hastelloy X tubular filters for H2 selective supported Pd–Ag alloy membranes preparation, Int. J. Hydrogen Energy 47 (66) (Aug. 2022) 28505–28517, https://doi.org/10.1016/J.IJHYDENE.2022.06.164.
[27] N. Xu, S. Ryi, A. Li, J.R. Grace, J. Lim, T. Boyd, Improved pre-treatment of porous stainless steel substrate for preparation of Pd-based composite membrane, Can. J. Chem. Eng. 91 (10) (2013) 1695–1701, https://doi.org/10.1002/cjce.21793.
[28] J.A. Calles, R. Sanz, D. Alique, Influence of the type of siliceous material used as intermediate layer in the preparation of hydrogen selective palladium composite membranes over a porous stainless steel support, Int. J. Hydrogen Energy 37 (7) (2012) 6030–6042, https://doi.org/10.1016/j.ijhydene.2011.12.164.
[29] E. Fernandez, et al., Preparation and characterization of metallic supported thin Pd–Ag membranes for hydrogen separation, Chem. Eng. J. 305 (2016) 182–190, https://doi.org/10.1016/j.cej.2015.09.119.
[30] S. Agnolin, et al., Development of selective Pd–Ag membranes on porous metal filters, Int. J. Hydrogen Energy (Apr. 2023), https://doi.org/10.1016/J.IJHYDENE.2023.03.306.
[31] W.H. Chen, K.H. Chen, J.K. Kuo, A. Saravanakumar, K.W. Chew, Optimization analysis of hydrogen separation from an H2/CO2 gas mixture via a palladium membrane with a vacuum using response surface methodology, Int. J. Hydrogen Energy 47 (100) (Dec. 2022) 42266–42279, https://doi.org/10.1016/J.IJHYDENE.2021.11.179.
[32] W.H. Chen, K.H. Chen, R.Y. Chein, H.C. Ong, K.D. Arunachalam, Optimization of hydrogen enrichment via palladium membrane in vacuum environments using Taguchi method and normalized regression analysis, Int. J. Hydrogen Energy 47 (100) (Dec. 2022) 42280–42292, https://doi.org/10.1016/J.IJHYDENE.2022.01.060.
[33] X. Han, et al., Optimization of the hydrogen production process coupled with membrane separation and steam reforming from coke oven gas using the response surface methodology, Int. J. Hydrogen Energy 48 (67) (Aug. 2023) 26238–26250, https://doi.org/10.1016/J.IJHYDENE.2023.03.222.
[34] Y. Orooji, E. Ghasali, N. Emami, F. Noorisafa, A. Razmjou, ANOVA design for the optimization of TiO2 coating on polyether sulfone membranes, Molecules 24 (16) (2019), https://doi.org/10.3390/molecules24162924.
[35] F. Xiangli, W. Wei, Y. Chen, W. Jin, N. Xu, Optimization of preparation conditions for polydimethylsiloxane (PDMS)/ceramic composite pervaporation membranes using response surface methodology, J. Memb. Sci. 311 (1–2) (Mar. 2008) 23–33, https://doi.org/10.1016/J.MEMSCI.2007.11.054.
[36] M. Khayet, M.N.A. Seman, N. Hilal, Response surface modeling and optimization of composite nanofiltration modified membranes, J. Memb. Sci. 349 (1–2) (Mar. 2010) 113–122, https://doi.org/10.1016/J.MEMSCI.2009.11.031.
[37] D.A. Pacheco Tanaka, et al., Preparation of palladium and silver alloy membrane on a porous α-alumina tube via simultaneous electroless plating, J. Memb. Sci. 247 (1–2) (2005) 21–27, https://doi.org/10.1016/j.memsci.2004.06.002.
[38] E. Fernandez, et al., Development of thin Pd–Ag supported membranes for fluidized bed membrane reactors including WGS related gases, Int. J. Hydrogen Energy 40 (8) (Mar. 2015) 3506–3519, https://doi.org/10.1016/J.IJHYDENE.2014.08.074.
[39] S.N. Paglieri, J.D. Way, Innovations in palladium membrane research, Sep. Purif. Methods 31 (1) (2002) 1–169, https://doi.org/10.1081/SPM-120006115.
[40] J.H. Lee, J.Y. Han, K.M. Kim, S.K. Ryi, D.W. Kim, Development of homogeneous Pd–Ag alloy membrane formed on porous stainless steel by multi-layered films and Ag-upfilling heat treatment, J. Memb. Sci. 492 (Oct. 2015) 242–248, https://doi.org/10.1016/J.MEMSCI.2015.04.029.
[41] Y.-H. Chi, P.-S. Yen, M.-S. Jeng, S.-T. Ko, T.-C. Lee, Preparation of thin Pd membrane on porous stainless steel tubes modified by a two-step method, Int. J. Hydrogen Energy 35 (12) (Jun. 2010) 6303–6310, https://doi.org/10.1016/j.ijhydene.2010.03.066.
[42] M.E. Ayturk, I.P. Mardilovich, E.E. Engwall, Y.H. Ma, Synthesis of composite Pd-porous stainless steel (PSS) membranes with a Pd/Ag intermetallic diffusion barrier, J. Memb. Sci. 285 (1–2) (Nov. 2006) 385–394, https://doi.org/10.1016/J.MEMSCI.2006.09.008.
[43] D.A. Pacheco Tanaka, M.A. Llosa Tanco, J. Okazaki, Y. Wakui, F. Mizukami, T. M. Suzuki, Preparation of 'pore-fill' type Pd-YSZ-γ-Al2O3 composite membrane supported on α-Al2O3 tube for hydrogen separation, J. Memb. Sci. 320 (1–2) (2008) 436–441, https://doi.org/10.1016/j.memsci.2008.04.044.
[44] R.A. Fisher, The Design of Experiments, Oliver & Boyd, Oxford, England, 1935.
[45] R.A. Fisher, Statistical methods for research workers. Rev, eleventh ed., Oliver and Boyd, Edinburgh, 1925.
[46] M.B. Brown, A.B. Forsythe, The small sample behavior of some statistics which test the equality of several means, Technometrics 16 (1) (Feb. 1974) 129–132, https://doi.org/10.1080/00401706.1974.10489158.
[47] A. Bathke, The ANOVA F test can still be used in some balanced designs with unequal variances and nonnormal data, J. Stat. Plan. Inference 126 (2) (2004) 413–422, https://doi.org/10.1016/j.jspi.2003.09.010.
[48] M.J. Blanca, R. Alarcón, J. Arnau, R. Bono, R. Bendayan, Datos no normales: ¿es el ANOVA una opción válida? Psicothema 29 (4) (2017) 552–557, https://doi.org/10.7334/psicothema2016.383.
[49] B. Lantz, The impact of sample non-normality on ANOVA and alternative methods, Br. J. Math. Stat. Psychol. 66 (2) (2013) 224–244, https://doi.org/10.1111/j.2044-8317.2012.02047.x.
[50] A.S.S. Shapiro, M.B. Wilk, Biometrika Trust an analysis of variance test for normality (Complete samples) Published by: Oxford University press on behalf of Biometrika trust stable, Biometrika 52 (3) (1965) 591–611 [Online]. Available: https://pdfs.semanticscholar.org/1f1d/9a7151d52c2e26d35690dbc7ae8098beee22.pdf.
[51] H. Levene, "Robust Tests for Equality of Variances," Contrib. To Probab. Stat. Essays Honor Harold Hotell., no. Stanford University Press, pp. 278–292.
[52] R Core Team, No Title," *R: A Language and Environment for Statistical Computing*, R Foundation for Statistical Computing, Vienna, Austria, 2022 [Online]. Available: https://www.r-project.org/.
[53] S. Agnolin, L. Di Felice, A.P. Tanaka, M.L. Tanco, W.J.R. Ververs, F. Gallucci, "Intensification of hydrogen production: Pd–Ag membrane on tailored hastelloy-X filter for membrane-assisted steam methane reforming,", Processes 12 (1) (2024) https://doi.org/10.3390/pr12010040.
[54] S. Nayebossadri, S. Fletcher, J.D. Speight, D. Book, Hydrogen permeation through porous stainless steel for palladium-based composite porous membranes, J. Memb. Sci. 515 (Oct. 2016) 22–28, https://doi.org/10.1016/J.MEMSCI.2016.05.036.
[55] S.C. Chen, G.C. Tu, C.C.Y. Hung, C.A. Huang, M.H. Rei, Preparation of palladium membrane by electroplating on AISI 316L porous stainless steel supports and its use for methanol steam reformer, J. Memb. Sci. 314 (1–2) (Apr. 2008) 5–14, https://doi.org/10.1016/J.MEMSCI.2007.12.066.
[56] M. Chotirach, S. Tantayanon, S. Tungasmita, K. Kriausakul, Zr-based intermetallic diffusion barriers for stainless steel supported palladium membranes, J. Memb. Sci. 405–406 (Jul. 2012) 92–103, https://doi.org/10.1016/J.MEMSCI.2012.02.055.
[57] S. Samingprai, S. Tantayanon, Y.H. Ma, Chromium oxide intermetallic diffusion barrier for palladium membrane supported on porous stainless steel, J. Memb. Sci. 347 (1–2) (Feb. 2010) 8–16, https://doi.org/10.1016/J.MEMSCI.2009.09.058.

[58] S.K. Ryi, et al., Electroless plating of Pd after shielding the bottom of planar porous stainless steel for a highly stable hydrogen selective membrane, J. Memb. Sci. 467 (Oct. 2014) 93–99, https://doi.org/10.1016/J.MEMSCI.2014.04.058.
[59] S.K. Ryi, J.S. Park, S.H. Kim, D.W. Kim, K. Il Cho, Formation of a defect-free Pd–Cu–Ni ternary alloy membrane on a polished porous nickel support (PNS), J. Memb. Sci. 318 (1–2) (Jun. 2008) 346–354, https://doi.org/10.1016/J.MEMSCI.2008.02.055.
[60] A. Bottino, et al., Sol-gel synthesis of thin alumina layers on porous stainless steel supports for high temperature palladium membranes, Int. J. Hydrogen Energy 39 (9) (2014) 4717–4724, https://doi.org/10.1016/j.ijhydene.2013.11.096.
[61] C. Mateos-Pedrero, M.A. Soria, I. Rodríguez-Ramos, A. Guerrero-Ruiz, Modifications of Porous Stainless Steel Previous to the Synthesis of Pd Membranes, vol. 175, Elsevier Masson SAS, 2010.
[62] A. Tarditi, C. Gerboni, L. Cornaglia, PdAu membranes supported on top of vacuum-assisted ZrO2-modified porous stainless steel substrates, J. Memb. Sci. 428 (Feb. 2013) 1–10, https://doi.org/10.1016/J.MEMSCI.2012.10.029.
[63] M.L. Bosko, F. Ojeda, E.A. Lombardo, L.M. Cornaglia, NaA zeolite as an effective diffusion barrier in composite Pd/PSS membranes, J. Memb. Sci. 331 (1–2) (Apr. 2009) 57–65, https://doi.org/10.1016/J.MEMSCI.2009.01.005.
[64] A. Arratibel, A. Pacheco Tanaka, I. Laso, M. van Sint Annaland, F. Gallucci, Development of Pd-based double-skinned membranes for hydrogen production in fluidized bed membrane reactors, J. Memb. Sci. 550 (August 2017) (2018) 536–544, https://doi.org/10.1016/j.memsci.2017.10.064.
[65] F. Guazzone, E.E. Engwall, Y.H. Ma, Effects of surface activity, defects and mass transfer on hydrogen permeance and n-value in composite palladium-porous stainless steel membranes, Catal. Today 118 (1–2) (2006) 24–31, https://doi.org/10.1016/j.cattod.2005.12.010.
[66] I.P. Mardilovich, E. Engwall, Y.H. Ma, Dependence of hydrogen flux on the pore size and plating surface topology of asymmetric Pd-porous stainless steel membranes, Desalination 144 (1–3) (Sep. 2002) 85–89, https://doi.org/10.1016/S0011-9164(02)00293-X.
[67] X. Li, A. Li, C.J. Lim, J.R. Grace, Hydrogen permeation through Pd-based composite membranes: effects of porous substrate, diffusion barrier and sweep gas, J. Memb. Sci. 499 (Feb. 2016) 143–155, https://doi.org/10.1016/J.MEMSCI.2015.10.037.